Quantum criticality in NbFe_{2} induced by zero carrier velocity

Brian P. Neal, Erik R. Ylvisaker, and Warren E. Pickett

Phys. Rev. B **84**, 085133 — Published 29 August 2011

DOI: 10.1103/PhysRevB.84.085133

Zero Carrier Velocity Induced Quantum Criticality in $NbFe_2$

Brian P. Neal,[1] Erik R. Ylvisaker,[1] and Warren E. Pickett[1]

[1]*Department of Physics, University of California Davis*

The transition metal intermetallic compound $NbFe_2$ displays a magnetic quantum critical point very near stoichiometry, unlike other Fe-based intermetallics, and no field or pressure tuning is required. In this compound we obtain an obvious candidate for the origin of quantum criticality: an accidental Fermi surface "hot stripe" centered on a point of vanishing quasiparticle velocity on the Fermi surface at an unconventional band critical point (uBCP) of $NbFe_2$. Around this uBCP the dispersion is cubic ($\varepsilon_k - \varepsilon_F \propto k_x^3$) in one direction in the hexagonal basal plane and has a saddle point character in the orthogonal k_y, k_z plane; both aspects have significant consequences. At such a uBCP Moriya's theory of weak magnetism breaks down due to divergent contributions to the dynamic bare susceptibility from the uBCP, both at $Q \to 0$ and at momenta spanning the uBCPs. These results are reminiscent of an earlier suggestion that anomalously low Fermi velocities are in essential aspect of the incipient or weak ferromagnetism of $TiBe_2$, and strongly support the viewpoint that, for some quantum critical points, the mechanism may be identifiable in the underlying (mean field) electronic structure.

PACS numbers:

I. BACKGROUND

Quantum phase transitions, and the quantum critical (QC) behavior displayed near these transitions, arise from quantum, rather than thermal, fluctuations, which involve the lowest energy excitations of the material. In metals, these excitations lie at the Fermi surface, and require some peculiar feature: competing interactions, an unusual Fermi surface feature, or anomalous near-zero-energy fluctuations of another origin, to drive the transition and to give rise to the quantum critical behavior around the critical point. A number of quantum critical materials have been discovered experimentally and in some cases have been studied in great detail. Competing (magnetic) interactions are often suspected to be the source of criticality. Rarely has any Fermi surface feature been identified as clearly responsible for quantum criticality, possibly because most QC metals are strongly correlated systems whose Fermi surfaces, hence their low energy band structures, may not be given precisely enough by the available mean field band theories. An exception to this is the high temperature superconducting cuprates, where an extended van Hove singularity has received attention. Such singularities have been studied extensively, both in weak coupling[1] and in the Hubbard model at strong coupling.[2–4]

$Nb_{1-x}Fe_{2+x}$ is a rare example of an itinerant transition metal intermetallic compound displaying antiferromagnetic quantum criticality. Its unusual magnetic behavior and its sensitivity to off-stoichiometry (Nb deficiency x) has been known for over two decades,[5,6] and its phase diagram and low temperature (T), small x behavior has recently been clarified.[7–9] At stoichiometry, its susceptibility is Curie-Weiss-like down to the SDW transition (probably long wavelength) at T_{sdw}=10 K with vanishing Curie-Weiss temperature, reflecting antiferromagnetism (AF) in close proximity to a FM QCP. Strongly negative magnetoresistance and a metamagnetic transition around 0.5 Tesla (at 2 K) reflect the removal of strong magnetic fluctuations by a relatively small field. The QCP occurs at the small Nb excess of x_{cr} = -0.015, for which resistivity scaling as $T^{3/2}$ and linear specific heat coefficient $\gamma \propto$ ln T below 4 K reflect non-Fermi liquid behavior characteristic of a QCP. Even off stoichiometry the samples are rather clean (residual resistivity as low as[8] 5 $\mu\Omega$ cm) reflecting small disorder scattering. For $x < x_{cr}$ (Nb excess) and for $x > 0.008$ (Fe excess), ferromagnetic (FM) (including possibly ferrimagnetic [FiM]) order is observed.[8] This system has been featured in recent overviews of quantum criticality in weak magnets[10,11] suggesting that in searching for the mechanism of quantum criticality more emphasis should be given to transition metal compounds[12] (versus f-electron systems).

There is no viable explanation of why this particular itinerant system should display such unusual quantum criticality, and this is the question we address here. The most detailed theories of quantum criticality suppose that the physics is dominated by fluctuations around the critical point, and treat the effects of low energy fermionic excitations without specifically addressing their origin.[13–17] The shortcomings of current theories for itinerant quantum criticality have been re-emphasized recently.[18] A necessary assumption is an underlying well behaved systems of non-interacting fermions. Imada *et al.*[19] have suggested itinerant quantum criticality arises either from proximity to a first-order transition (quantum tricriticality), a metal-insulator transition (not the case here), or a Lifshitz transition, which accompanies a change in topology of the Fermi surface. Frustration of magnetic order on the Fe2 Kagome sublattice has also been suggested as playing a part.[20] The study of interacting systems near conventional band critical points (BCPs) (van Hove singularities) indicates non-Fermi liquid behavior[1] and a profusion of possible phases.[21] Stronger

singularities may be expected to further complicate the phase diagram.

II. STRUCTURAL AND CALCULATIONAL DETAILS

$NbFe_2 \equiv NbFe1_{0.5}Fe2_{1.5}$ forms in the hexagonal Laves phase C14 space group $P6_3/mmc$ (#194), with Nb at $4f$ $(\frac{1}{3}, \frac{2}{3}, u)$ which can be considered to lie within Fe cages, Fe1 at $2a$ (0,0,0) which lies on a hexagonal sublattice, and Fe2 at $6h$ $(v,2v,\frac{3}{4})$ sites that form Kagome lattice sheets in the basal plane. We perform all calculations with the experimental lattice constants $a = 4.841$ Å, $c = 7.897$ Å, and relaxed internal parameters $u = 0.0652$, $v = 0.1705$, using the full potential local orbital code[22] with k-point meshes up to $57 \times 57 \times 55$ to map out the unusual part of the band structure in detail. The full potential LAPW code Wien2k[23] has been used to check consistency of the fine details that we discuss.

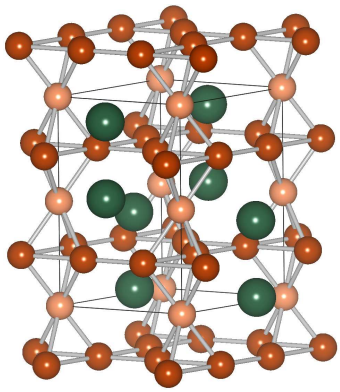

FIG. 1: Crystal structure of $NbFe_2 = NbFe1_{0.5}Fe2_{1.5}$, with hexagonal space group $P6_3/mmc$ (#194). The Fe2 sites lie on a Kagome lattice (e.g. the upper and lower atomic planes in this figure), the Fe1 sites lies on a simple triangular lattice midway between Fe2 layers, and Nb atoms occupy "interstitial" sites.

III. ELECTRONIC ANOMALY

The electronic structure of $NbFe_2$ was studied initially by Takayama and Shimizu,[24] and more recently by Subedi and Singh (SS).[25] The complex band structure (due to 12 transition metal atoms in the unit cell) is shown in the basal plane in a 2 eV region centered on the Fermi energy (E_F) in Fig. 2. The Fermi level lies on the upper (steeply decreasing) density of states (DOS) peak, shown on a fine energy scale in Fig. 2(b), with several bands crossing E_F.

The Fermi surfaces are correspondingly many and varied, and have been presented and discussed by Tompsett and coworkers.[26] The point we will emphasize here is the wiggle in the band just crossing E_F along the Γ-M direction that produces an unusually flat portion only 6 meV (equivalent to 70 K temperature) above E_F. We argue that, when the Fermi level is tuned to this critical point, the vanishing velocity in this critical region produces unusual low energy electronic excitations that can account for anomalous behavior, *viz.* a quantum critical point at a low doping level, as is observed in $NbFe_2$ (x_{cr} = -0.015).

This viewpoint has received strong support from alloy calculations (using the coherent potential approximation [CPA]) by Alam and Johnson.[27] They find that CPA results place the Fermi level at this uBCP at $x = -0.0174$, extremely close to the experimental concentration at the critical point. The dispersion remains well represented by cubic along the symmetry direction.

Referencing the energy and wavevector to the point of the anomaly, the uBCP dispersion is given to lowest order along each axis by

$$\varepsilon_k = \frac{k_x^3}{3m_e K} + \frac{k_y^2}{2m_y} - \frac{k_z^2}{2m_z}, \tag{1}$$

i.e. it is effective-mass-like along k_y and k_z with opposite signs of the masses m_y, m_z, but it is infinitely massive along the k_x direction, with cubic rather than quadratic variation. (The calculated band is even flatter than this

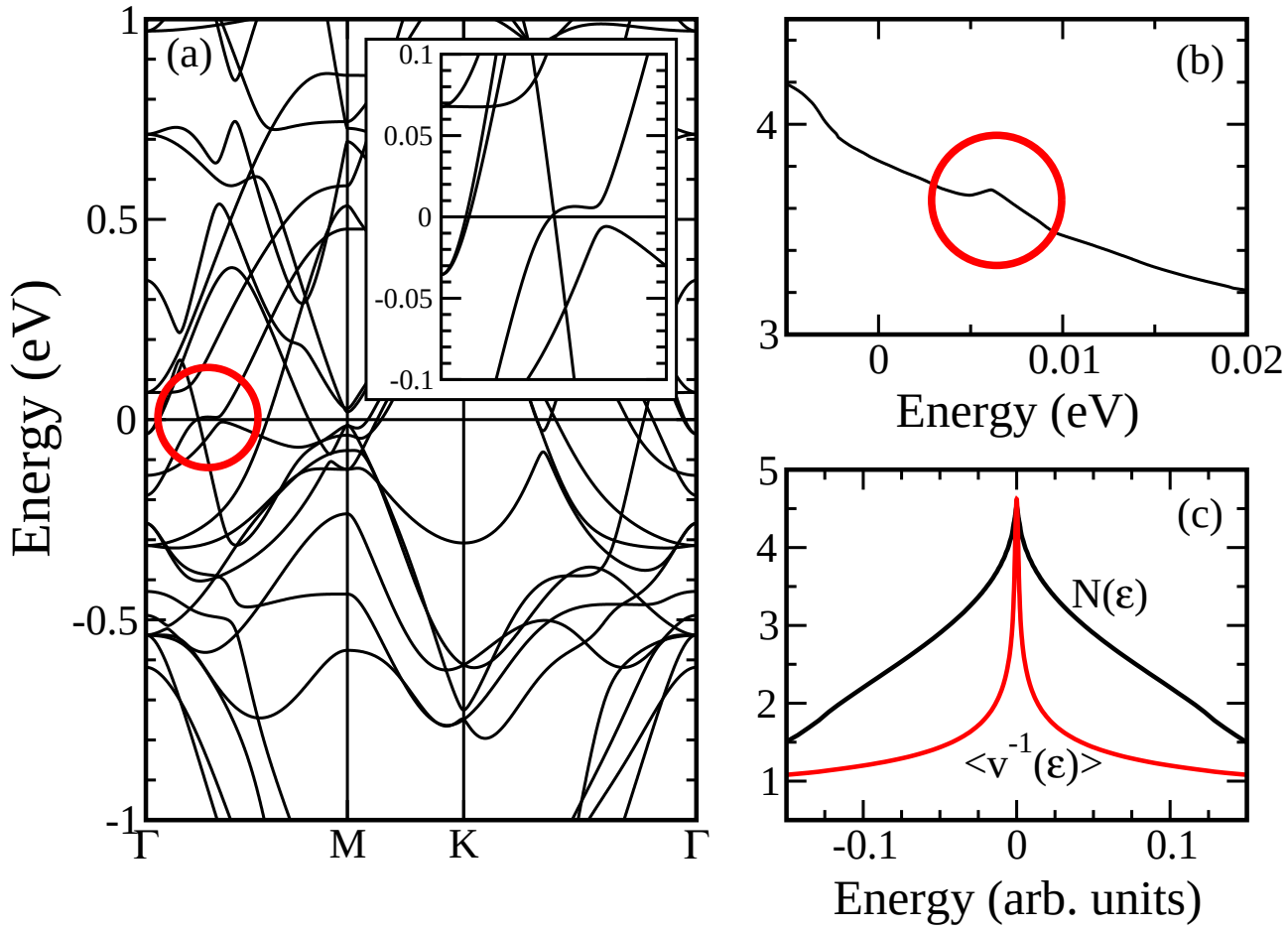

FIG. 2: (a) Band structure of $NbFe_2$ within 1 eV of the Fermi level. The inset shows the band critical point 6 meV above E_F that lies one-third of the way along the Γ-M line. (b) The DOS of $NbFe_2$ near E_F on a fine scale, showing the steeply decreasing DOS in the region of E_F. The circle indicates the position in energy of the uBCP, 6 meV above E_F, calculated without the precision necessary to establish the shape of the anomaly (in spite of the fine k-mesh we have used). (c) A high resolution calculation (in arbitrary units) in the uBCP region of the behavior of N(E) (upper black curve), and indicating the divergence of the inverse velocity $\langle v^{-1}(E)\rangle$ (lower red curve), which is a fundamental quantity in Moriya's theory of weak magnetism.

approximation.) We characterize this dispersion through a quantity K with dimension of wavevector, corresponding heuristically to a k_x-dependent mass enhancement K/k_x, diverging as $k_x \to 0$. The crossing bands have nearly pure Fe2 d_{xz}, d_{yz} character (the Kagome sublattice), not involving either Fe1 or Nb orbitals.

This anomalous dispersion is an accidental occurrence (not related to symmetry or normal band edges), resulting from the crossing of two bands having the same symmetry that occurs extremely near the Fermi level of stoichiometric $NbFe_2$. Its distinctive character is evident by noting that the change in the constant energy surfaces near E=0 does not fit into the conventional categorization.[30] Because it is accidental, it requires tuning to put E_F exactly at the critical point, and the value x_{cr} of $NbFe_2$ is of the right magnitude to provide this tuning [$N(E_F)\times$ 6 meV = 0.02 electrons/f.u.]. For non-stoichiometry in a compound of two such different atoms as Nb and Fe, the direction of change of the Fermi level is not obvious *a priori*. However, alloy calculations can determine the Fermi level change with concentration, and new results by Alam and Johnson[27] have determined that indeed the uBCP lies at the Fermi level for $x = x_{cr}$. We proceed to examine the consequences for low energy excitations.

The Fermi energy E_F lies in a region of steeply decreasing density of states (DOS) (the full DOS has been presented by Takayama and Shimizu[24] and by Subedi and Singh (SS)[25]), corresponding to the gaps that open in much of the zone (along K-H, along L-H-A). The DOS near E_F is displayed in Fig. 2b and gives an idea of the magnitude of the peak at the uBCP; the form for the dispersion in Eq. 1 is given more precisely in Fig. 2c.

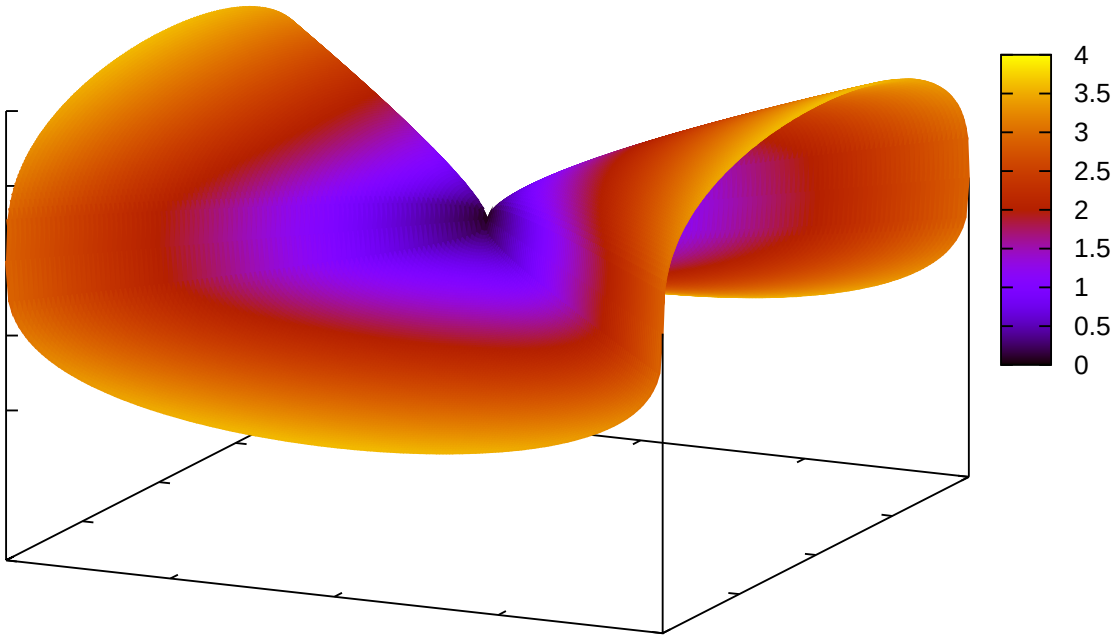

FIG. 3: Fermi surface (constant energy E=0) around the uBCP (see text), which lies at the center of the plot where the velocity vanishes; the anomalous k_x direction is plotted vertically. The color map indicates the relative velocity; the $\vec{k}$, energy, and velocity scales are arbitrary.

IV. EFFECT OF UNCONVENTIONAL BCP

The occurrence of BCPs (vanishing velocity) was first studied systematically by van Hove,[28] who noted that, in the absence of restrictions, BCPs in a band occur at most at isolated points. He studied the conventional (cBCP) case where the determinant of the Hessian $\nabla_k \nabla_k \varepsilon_k$ evaluated at the BCP is non-vanishing, which corresponds to vanishing velocity at (1) band edges, where the constant energy surface also vanishes, and (2) saddle points, with $\vec{v} = 0$ on a pinched-off surface. For our representation of the uBCP in $NbFe_2$, this *determinant vanishes* due to the cubic variation with k_x, resulting in this unconventional type of BCP. This uBCP therefore does not correspond to the usual possibilities, which are a (dis)appearing of a Fermi surface or to a pinching off of the Fermi surface.

Instead, it is an isolated vanishing of carrier velocity on an extended surface, which is shown in Fig. 3. A spectrum of soft excitations (arbitrarily low velocities on the Fermi surface), vanishing more conventionally (linearly) in the k_y and k_z directions, is joined by a line of quadratically vanishing velocities off the Fermi surface along the k_x direction. The anomaly in the DOS is shown in Fig. 2c and numerically appears to behave roughly as $-|E|^{2/3}$ near the peak. The behavior of $\langle v^{-1}(E) \rangle$, whose importance is discussed below, is also shown, and is fit well with a $E^{-\frac{1}{4}}$ *divergence.*

A. Comments on zero Fermi velocity

The occurrence of a zero Fermi velocity has not attracted much attention to date. The constant energy E surface $\mathcal{S}_E$ is given by $\varepsilon_k = E$, *i.e.* one condition on a function of three variables. For constant velocity surfaces, we consider

the surfaces of constant v_k^2, which (unlike $|\vec{v}_k|$) is an analytic function of k except at degeneracies (including band crossings) which is not our interest here. The constant velocity surface $\mathcal{S}_V$ given by $v_k^2 = V^2$ is another surface in k-space that may intersect the E surface, so constant velocities form lines (contours) on $\mathcal{S}_E$. This picture suggests that zero velocities might arise as lines on the Fermi surface.

However, vanishing velocity $v_k^2 = 0$ is special. The constant velocity surface $\mathcal{S}_V$ arises from a single condition:

$$v_{k,x}^2 = V - v_{k,y}^2 - v_{k,z}^2, \tag{2}$$

implicitly giving the surface $k_x(k_y, k_z; V)$ in k-space. The case V=0 is special because it requires requires separately $v_{k,x} = v_{k.y} = v_{k,z} = 0$, *i.e.* three conditions. One condition leads to a surface, two conditions leads to a line, so three conditions reduce to a point. For a point to lie on a separate surface is an accidental, albeit tunable, occurrence.

The conditions for $\mathcal{S}_E$ and $\mathcal{S}_V$ described above do not take into account any connection between the two surfaces, whereas $\vec{v}_k$ being the derivative of ε_k is the case of interest. Is this relevant? On an $\mathcal{S}_E$ surface, the velocity is always normal to the surface, so at a given point $\vec{k}$ on $\mathcal{S}_E$, the velocity is given not by a general vector but by a signed scalar: positive if outward, negative if inward. Vanishing velocity however still requires three conditions: the orientation of the surface normal (two angles) and the vanishing of the magnitude. Thus from this viewpoint as well as the former one, it follows that zero velocities occur at most as isolated points on the Fermi surface.

B. Velocity distribution around the uBCP

Going beyond averages over the FS and the bare susceptibility, the *spectrum* of carrier velocities (hence, single-particle and pair excitation energies) is of fundamental concern for spin fluctuations and quantum criticality. We have evaluated the distribution of velocities V at given energy $\mathcal{E}$, as done earlier for $TiBe_2$,[29] for the uBCP

$$D(\mathcal{E}, V) = \sum_k \delta(\varepsilon_k - \mathcal{E})\delta(|\vec{v}_k| - V), \tag{3}$$

and display the results in Fig. 4. For isotropic free electrons this distribution vanishes except for a highly singular value along the line $V = \sqrt{2m\mathcal{E}}$, where it becomes the product of two δ-functions. For the uBCP, the small V region of $D(\mathcal{E}, V)$ is sharply peaked in the vicinity of $V_m(E) \propto \mathcal{E}^{2/3}$, arising from the quadratically small velocity along the x-axis with relatively large phase space. The spectrum vanishes at smaller velocities $V < V_m$, but has a tail at higher velocities where the other two axes contribute.

The Fermi surface topology near the uBCP is given (for simplicity, scaling out the masses and the coefficient K to get $\varepsilon_k = k_x^3 + k_y^2 - k_y^2$) from $\varepsilon_k = 0$ by

$$k_x = \mathrm{sgn}(k_y^2 - k_z^2)|k_y^2 - k_z^2|^{1/3}. \tag{4}$$

This warped FS (Fig. 3) is centered on the peculiar singular uBCP. As the uBCP is approached, the FS tangent plane becomes sensitively dependent on the angle of approach, and the curvature becomes singular. Such a zero velocity point leads to arbitrarily low energy single-particle excitations around the uBCP, including a "hot stripe" of low velocities just off the Fermi surface along the $\pm k_x$ axes (where $v_k \sim k_x^2$ is quadratic, not linear, in k) whose impact on magnetic fluctuations requires investigation.

C. Coefficient in Moriya theory

In Moriya's widely applied theory[15] of nearly FM (and AF) metals, the small-Q inverse susceptibility has an imaginary part at low energy given by $N(E_F)\langle v^{-1}\rangle\omega/Q$. It is straightforward to show that when there is a BCP on a (non-vanishing) FS, $\langle v^{-1}\rangle$ diverges. The expression is

$$\langle v^{-1}\rangle = \sum_k \frac{1}{v_k}\delta(\varepsilon_k) \propto \int_S \frac{dS_k}{v_k^2}. \tag{5}$$

Since v_k^2 is smooth and assuming a minimum (vanishing) at k_0 (v_{k_0}=0), the Taylor expansion is

$$v_k = \frac{1}{2}\vec{\kappa}\cdot\mathbf{G}\cdot\vec{\kappa} + ... \tag{6}$$

where $\vec{\kappa} \equiv \vec{k} - \vec{k}_0$. The second derivative matrix $\mathbf{G}$ can, without loss of generality, be taken to be diagonal and with wavevector rescaling, $\mathbf{G} \to g\mathbf{I}$. Then in a small region $\kappa < k_1$ where the Taylor expansion holds, the contribution to $\langle v^{-1} \rangle$ when $v_{k_0} = 0$ is

$$\langle v^{-1} \rangle \propto g^{-1} \int_0^{k_1} \frac{2\kappa d\kappa}{\kappa^2} \sim \frac{2}{g} log(\kappa) \tag{7}$$

giving an infrared divergence at the lower limit of integration. From Fig. 2c, numerical scaling gives $\langle v^{-1}(E) \rangle \sim E^{-1/4}$ for this form of uBCP. This divergence means that Moriya's theory as currently formulated breaks down as this uBCP approaches the Fermi surface, and requires generalization: a higher order expansion of the non-interacting susceptibility is required.

If the dispersion expansion Eq. 1 holds up to k_m (perhaps a few percent of the Brillouin zone dimension) we obtain (in the limit $\omega/Q^2 \to 0$ followed by $Q \to 0$)

$$\begin{aligned} \chi^\circ(Q,\omega) &= \sum_k \frac{f(\varepsilon_k) - f(\varepsilon_{k+Q})}{\varepsilon_{k+Q} - \varepsilon_k - \omega + i\eta} \\ &\to \bar{\chi}^\circ(Q) + \sum_{k<k_m} \frac{\sum_j \frac{Q_j^2}{2m(k)_j}}{\sum_j \frac{Q_j^2}{2m(k)_j} - \omega + i\eta} \delta(\varepsilon_k), \end{aligned} \tag{8}$$

where the first term $\bar{\chi}^\circ(Q)$ arises from $|\vec{k}| > k_m$ and is essentially that presented by SS, and the second term arises from the uBCP region where the *quadratic* term replaces the usual $\vec{Q} \cdot \vec{v}_k$ term. Here η is an infinitesimal and the masses $m(k)_j$ along the three axes are ($m_e K/k_x$, m_y, -m_z).

Neglecting the k_x dependence, which due to its smallness is unimportant for most directions of $\vec{Q}$, in the integrand for $k < k_m$ for the real part leads to a contribution to the bare fluctuation spectrum from the uBCP given by

$$\begin{aligned} \Delta\chi^\circ(Q,\omega) &\approx \Delta N(E_F) \frac{Q_y^2/2m_y - Q_z^2/2m_z}{Q_y^2/2m_y - Q_z^2/2m_z - \omega} \\ &- i\pi\omega \sum_{k<k_m} \delta(\varepsilon_k) \delta\left(\frac{3k_x Q_x^2}{m_e K} - \left[\frac{Q_y^2}{2m_y} - \frac{Q_z^2}{2m_z} \right] \right), \end{aligned} \tag{9}$$

where $\Delta N(E_F)$ is the DOS from within $k < k_m$. Due to the saddle point character in the $k_y - k_z$ plane, the real part has strong anisotropy including sign changes for $|Q_y^2/2m_y - Q_z^2/2m_z| \leq \omega$ that do not occur for conventional bands. The imaginary part acquires a low energy form

$$\mathrm{Im}\Delta\chi^\circ(Q,\omega) = \frac{\omega}{Q_x^2} \bar{C}_Q, \tag{10}$$

where $\bar{C}_Q$ is a somewhat $\vec{Q}$-dependent amplitude arising from an integral over the line of constant k_x on the Fermi surface where the argument of the δ-function in Eq. (9) vanishes. This lowest order result for small ω, Q suggests that the temporal fluctuation ω/Q term in Moriya theory

$$\chi^\circ(Q,\omega)^{-1} = \bar{\chi}^{\circ,-1} + AQ^2 - iC\omega/Q + ... \tag{11}$$

must be replaced by

$$\chi^\circ(Q,\omega)^{-1} = \chi^\circ(0,0)^{-1} + AQ^2 - i\bar{C}_Q \frac{\omega}{Q_x^2} + ... \tag{12}$$

when there is an uBCP at or near the Fermi surface.

Thus the (bare) low energy magnetic fluctuation spectrum is no longer a simple function of $|\vec{Q}|$ and ω, rather it is highly and essentially *anisotropic* around the $|Q_y| = |Q_z|$ directions, no longer being a simple function of $|\vec{Q}|$ and ω, and the low energy dynamics are scaled by Q_x^2 rather than Q.. It will be important to learn how treatment of the fluctuations will renormalize this bare low energy behavior.

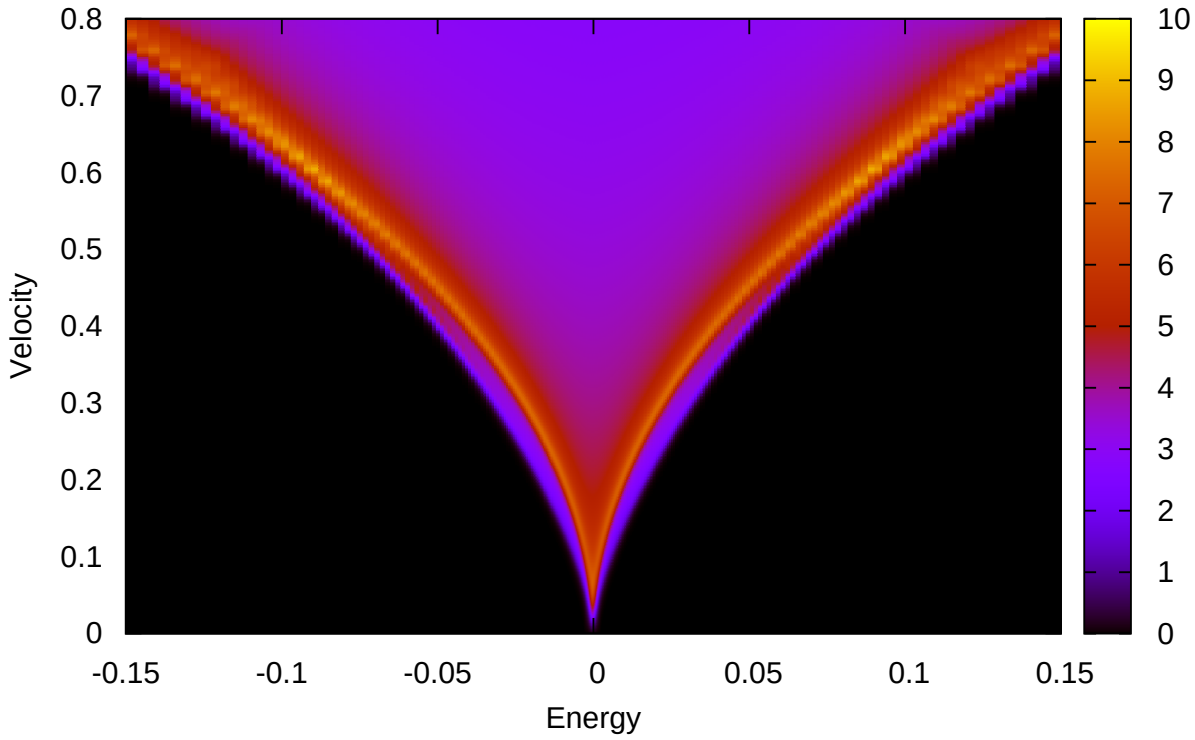

FIG. 4: Color plot representation of the velocity spectrum $D(\mathcal{E}, V)$, which provides the decomposition of velocities (vertical axis) for each energy (horizontal axis). All scales are arbitrary. The spectrum is sharply and narrowly peaked very near the onset, with a long tail at higher velocities.

D. Implications of Multiple uBCPs

So far we have only discussed the isolated uBCP, which would be most relevant to ferromagnetic, rather than antiferromagnetic, quantum criticality. In the hexagonal lattice there are six symmetry related such hot spots $K_c(\pm 1, 0), K_c(\pm\frac{1}{2}, \pm\frac{\sqrt{3}}{2})$, with $K_c \approx 0.30\ k_{zb}$ in terms of the zone boundary distance. There are therefore five non-zero spanning Q-vectors (and symmetry partners) spanning these hot spots, for which the large-Q susceptibility at zero or small energy will be correspondingly large, thus providing a driving force for spin-density waves (SDW) or AFM order at the corresponding wavevectors. Note that, quite generally, the $\omega \equiv 0$, $Q \to 0$ susceptibility approaches $\mathrm{N(E}_F)$, which also possesses a sharp, but modest in magnitude, peak at the BCP.

Thus both FM and AF (SDW) susceptibilities will be strongly enhanced, and thus will be competing for their own separate magnetic order. This competition introduces another type of frustrating fluctuations, the effects of which only a renormalized theory can resolve. For transitions between inversion related hot-spots the SDW susceptibility will be particularly large, since the hot stripe axes will then be aligned. These AFM wavevectors may require special attention.

V. FIXED SPIN MOMENT STUDY

The small Q, small ω susceptibility we have just examined reveals the delicate low energy tendencies of a nonmagnetic system with an uBCP. We next explore magnetic tendencies and the distribution of moments in $NbFe_2$ by performing fixed spin moment[34] (FSM) calculations. Magnetic states have been studied previously at stoichiometry by SS and for doped materials by Tompsett *et al.* Like the earlier studies, we do not pursue noncollinear magnetism here.

Our calculated energies $E(M)$ and atomic moments versus imposed moment M are presented in Fig. 5, using the experimental crystal structure parameters and the GGA exchange-correlation functional. Because in the absence of constraints the nonmagnetic state is calculated to be unstable to magnetic order (as observed), the curves are not symmetric around zero moment; however, there is always a symmetry related solution at negative M where all spin directions are reversed from the corresponding state at positive M.

Two magnetic states are evident in our series of calculations, a low net moment ferrimagnetic (FiM) arrangement and a (forced) ferromagnetic (FM) state. The more stable state is the FiM one with total moment of 0.4 μ_B (all moments are quoted per formula unit), comprised of moments of about 1 μ_B on Fe2 and -1.8 μ_B on Fe1. This state is the same configuration as the lowest energy configuration found by SS[25] (of five that they found). Their moments (-1.18 μ_B, 0.75 μ_B for Fe1, Fe2, respectively) differ from ours (-2 μ_B, 0.8 μ_B) indicating sensitivity to structure (they use theoretically relaxed internal positions) and exchange-correlation functional, as already noted by Tompsett *et al.* For the range of moments we have studied there is always a small negative moment (of the order of 0.1 μ_B or less) on the Nb atom. In the subsequent discussion, recall the atomic ratios are $NbFe1_{0.5}Fe2_{1.5}$.

As the imposed total moment is increased "adiabatically" (we use the spin densities from the previous fixed moment to begin self-consistency for the next in our FSM calculations), the moments on both Fe atoms initially change by comparable amounts along the direction of change in the imposed moment. In the vicinity of M=1.4 μ_B the decreased downward moment of Fe1 ($\sim 1\mu_B$) becomes unstable, and it flips direction in a first-order fashion to the FM state, where it rapidly approaches the same moment as Fe2. This first order "spin flop" transition is evident in the small discontinuities of the Fe2 and Nb moments. The energy curve reflects nearly quadratic increases relative to the minimum of each of the two states (FiM and FM), with switchover from one to the other again reflecting first order behavior.

The minimum energy of the FM state (total moment of 2.4 μ_B) occurs with moments of about 1.1 μ_B and 1.5 μ_B on the Fe1 and Fe2 atoms respectively. The energy of this state, which is also one of those discussed by SS, is 12 meV/f.u. higher than the FiM state in our calculations. The strong variation in moments with applied field (*i.e.* imposed moment) indicates itinerant character of the magnetism, in agreement with the conclusion of SS, based on the different values of atomic moments occurring in the five configurations that they studied. All of the calculated states (FM, AFM, or FiM), by SS, by Tompsett *et al.*, and by us, have much larger moments than seen experimentally, which is the common finding in weak (and incipient) ferromagnets and points to the dominant influence of magnetic fluctuations.

The FSM calculations, and the results of SS, establish there are many ordered collinear states at stoichiometry differing in energy by only $\sim$ 10-20 meV/f.u. Unlike in fluctuating systems, magnetism in mean field approximation (as from DFT calculations with static moments) is not very sensitive to small anomalies in the band structure, and FSM results at x_{cr} show little difference from those at nearby band fillings. The near degeneracy of several magnetic states, as well as the possibility of magnetic frustration on the Kagome Fe2 sublattice, raises the further possibility of non-collinear magnetism (including spiral and longitudinal SDW) as well. Such behavior can depend on the (complicated) FSs. SS found weak variation of the generalized non-interacting susceptibility (no matrix elements) in the $Q_z = 0.38\pi/c$ plane in $NbFe_2$. For the same function, Tompsett *et al.* found along both [1,0,0] and [0.1.0] directions a very sharp *minimum* as $Q \to 0$. Neither provides support for the importance of ferromagnetic fluctuations ($Q \to 0$), but some of the bands at the Fermi level are strongly differentiated in amounts of Nb, Fe1, and Fe2 character, so matrix elements will be important.

VI. SUMMARY

We have identified an unconventional band critical point in the band structure of $NbFe_2$ and have pursued the consequences when the Fermi energy is tuned to the critical point. We have demonstrated that fluctuations around an uBCP are essentially different – highly anisotropic, and differing in the Q, ω dependence – from what is assumed in the more conventional treatments of magnetic quantum critical points. The dynamic fluctuation spectrum changes qualitatively from that of a conventional band structure, and Moriya's formulation for weak ferromagnets requires adjustment. From our calculations and earlier ones, $NbFe_2$ displays several low-lying magnetically ordered states (as

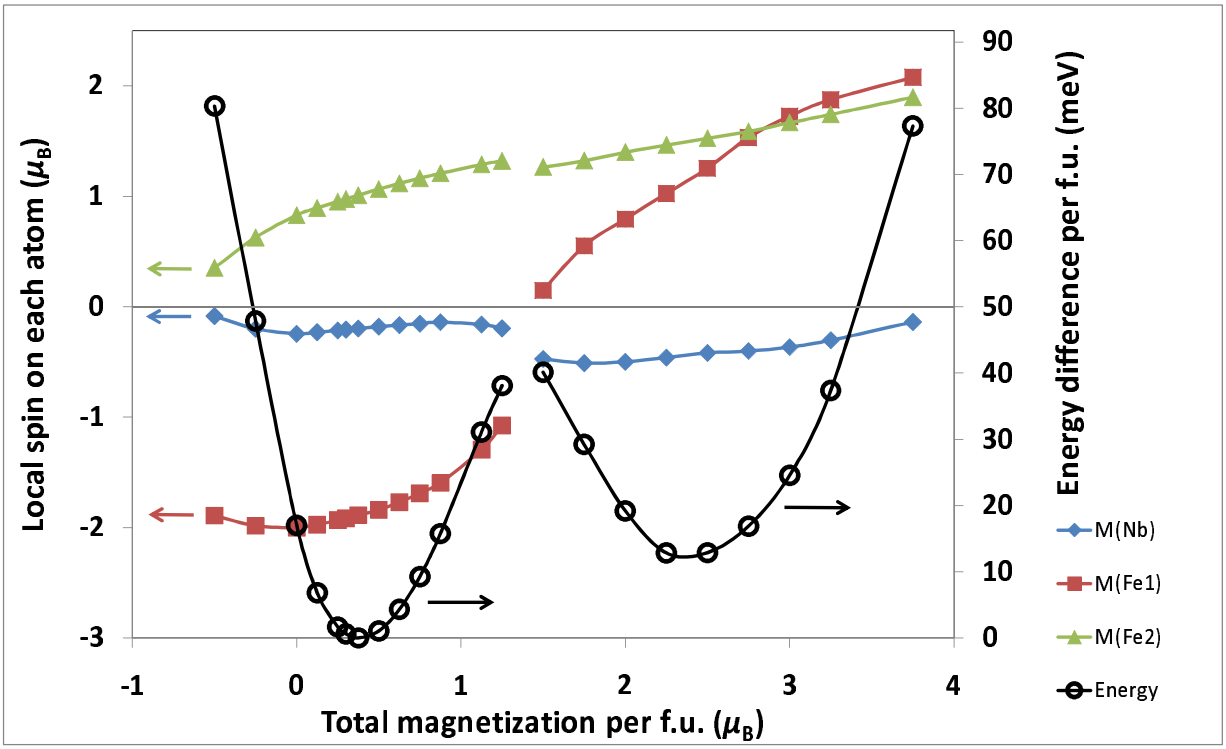

FIG. 5: Atomic moments (symbols) and energies (solid lines) from fixed spin moment studies, showing two distinct phases, ferrimagnetic (FiM) with minimum of energy around 0.3 μ_B/f.u., and ferromagnetic (FM) with minimum at 2.3 mu_B/f.u. The minima differ by 13 meV/f.u. Here M=0 corresponds to a zero net moment ferrimagnetic state, hence the curve is not symmetric around total moment M=0. The ferrimagnetic state could not be followed beyond M < -0.5 μ_B.

well as possibly non-collinear ones that have not yet been addressed), so the spectrum of low energy dynamic spin fluctuations may be unusually complex in this quantum critical material.

Two other intermetallics, both with the cubic (C15) Laves structure rather than the hexagonal (C14) Laves structure of $NbFe_2$, have attracted much attention due to their weak magnetism. $TiBe_2$ at stoichiometry is a highly enhanced paramagnetic that was long believed to have weak order because magnetic order appears in impure samples. van Hove singularities occur very near E_F in $TiBe_2$; if non-stoichiometry moves E_F upward by as little at 3 meV, the velocity spectrum[29] $D(E_F, V)$ extends nearly to V=0 and $\langle v^{-1} \rangle$ is enhanced by a factor of two. There is no uBCP as in $NbFe_2$, but the enhancement in low energy excitations (the occurrence of low velocities) bears similarity to $NbFe_2$. Weak magnetism and metamagnetic transitions in $ZrZn_2$ have been attributed[30] to a saddle point van Hove singularity (a cBCP) very near E_F. Ni_3Al (FM with small moment $< 0.1\mu_B/Ni$ below 40 K) and isovalent Ni_3Ga (highly enhanced but not ordered) have also attracted attention. The distinction was attributed by Aguayo *et al.*[31] to stronger spin fluctuations in Ni_3Ga, using analysis based on LDA results applied within Moriya theory. The band structure themselves are very similar except for one Al- (resp. Ga-)derived band, though there is no obvious anomaly in the band structure near E_F.

The $NbFe_2$ system, providing a rare example of itinerant, low temperature antiferromagnetism and non-Fermi liquid quasiparticle behavior at low temperature, seems to require a specific microscopic mechanism compared to the few other known weak itinerant magnets. We have proposed that an unconventional band critical point, in

which an isolated point of vanishing carrier velocity on an extended Fermi surface, provides the explanation. The self-consistent CPA calculations of Alam and Johnson[27] support this position of the Fermi level at the quantum critical point, implying further that the position of the critical point is not significantly renormalized by the critical fluctuations. Moriya's theory of weak magnetism requires generalization when the Fermi level lies near or at a uBCP, and the phenomenological renormalized Landau theory[32] that has been applied[33] to $ZrZn_2$ also must be generalized in this case. Generalizing the theory of itinerant quantum criticality to encompass such a uBCP should help to illuminate the mechanisms and the behavior around such itinerant QCPs.

We acknowledge K. Fredrickson who contributed to some of the calculations. This work was supported by DOE/SciDAC Grant No. DE-FC02-06ER25794 and by DOE grant DE-FG02-04ER46111.

[1] I. Dzyaloshinskii, J. Phys. I (France) **6**, 119 (1996).
[2] D. M. Newns, P. C. Pattnaik, and C. C. Tsuei, Phys. Rev. B **43**, 3075 (1991).
[3] K.-S. Chen, S. Pathak, S.-X. Yang, S.-Q. Su, D. Galanakis, K. Mikelsons, M. Jarrell, and J. Moreno, arXiv:1104.3261.
[4] S. Schmitt, arXiv.1005.3481.
[5] M. Shiga and Y. Nakamura, J. Phys. Soc. Japan **56**, 4040 (1087).
[6] Y. Yamada and A. Sakata, J. Phys. Soc. Japan **57**, 46 (1088).
[7] M. Brando *et al.*, Physica B **378-380**, 111 (2006).
[8] M. Brando *et al.*, Phys. Rev. Lett. **101**, 026401 (2008).
[9] D. Moroni-Klementowicz, M. Brando, C. Albrecht, and F. M. Grosche, in *CP850, Low Temperature Physics: 24th Intl. Conf. on Low Temperature Physics*, eds. Y. Takano, S. P. Hershfield, S. O. Hill, P. J. Hirschfeld, and A. M. Goldman (AIP, 2006), p. 1251.
[10] A. J. Schofield, Phys. Stat. Sol. B **247**, 563 (2010).
[11] W. J. Duncan *et al.*, Phys. Stat. Sol. B **247**, 544 (2010).
[12] P. Coleman, Phys. Stat. Sol. B **247**, 506 (2010).
[13] J. Hertz, Phys. Rev. B **14**, 1165 (1976).
[14] A. J. Millis, Phys. Rev. B **48**, 7183 (1993).
[15] T. Moriya, *Spin Fluctuations in Itinerant Electron Magnetism*, (Springer, Berlin, 1985).
[16] G. G. Lonzarich and L. Taillefer, J. Phys. C **18**, 4339 (1985).
[17] M. Vojta, Rep. Prog. Phys. **66**, 2069 (2003).
[18] C. Pfleiderer, S. R. Julian, and G. G. Lonzarich, Nature **414**, 427 (2001).
[19] M. Imada, T. Misawa, and Y. Yamaji, J. Phys.: Condens. Matter **22**, 164206 (2010).
[20] M. R. Crook and R. Cywinski, Hyperfine Interactions **85**, 203 (1994).
[21] A. P. Kampf and A. A. Katanin, Phys. Rev. B **67**, 125104 (2003).
[22] K. Koepernik and H. Eschrig, Phys. Rev. B **59**, 1743 (1999)
[23] K. Schwarz and P. Blaha, Comp. Mat. Sci. **28**, 259 (2003).
[24] N. Takayama and M.Shimizu, J. Phys. F: Met. Phys. **18**, L83 (1988).
[25] A. Subedi and D. J. Singh, Phys. Rev. B **81**, 024422 (2010); *erratum*, *ibid.* 059902(E) (2010).
[26] D. A. Tompsett, R. J. Needs, F. M. Grosche, and G. G. Lonzarich, Phys. Rev. B **82**, 155137 (2010).
[27] A. Alam and D. D. Johnson, private communication.
[28] L. van Hove, Phys. Rev. **89**, 1189 (1953).
[29] T. Jeong, A. Kyker, and W. E. Pickett, Phys. Rev. B **73**, 115106 (2006).
[30] Y. Yamaji, T. Misawa, and M. Imada, J. Phys. Soc. Japan **75**, 094719 (2006).
[31] A. Aguayo, I. I. Mazin, and D. J. Singh, Phys. Rev. Lett. **92**, 147201 (2004).
[32] M. Shimizu, Rep. Prog. Phys. **44**, 329 (1981).
[33] I. I. Mazin and D. J. Singh, Phys. Rev. B **69**, 020402 (2004).
[34] K. Schwarz and P. Mohn, J. Phys. F: Met. Phys. **49**, L129 (1984).